J Comput Aided Mol Des (2013) 27:173–184
DOI 10.1007/s10822-013-9636-8

Structural insights into the mechanism of translational inhibition by the fungicide sordarin

Biprashekhar Chakraborty · Raisa Mukherjee · Jayati Sengupta

Received: 13 July 2012 / Accepted: 25 January 2013 / Published online: 9 February 2013

Abstract The translational machinery has been found to be the target for a number of antibiotics. One such antibiotic sordarin selectively inhibits fungal translation by impairing the function of elongation factor 2 (eEF2) while being ineffective to higher eukaryotes. Surprisingly, sordarin is not even equally effective in impairing translation for all fungal species. The binding cavity of sordarin on eEF2 has been localized by X-ray crystallographic study and its unique specificity towards sordarin has been attributed to the species specific substitutions within a stretch of amino acids (sordarin specificity region, SSR) at the entrance of the cavity. In this study, we have analyzed the sordarin-binding cavity of eEF2 from different species both in isolated and ribosome-bound forms in order to decipher the mechanism of sordarin binding selectivity. Our results reveal that the molecular architecture as well as the microenvironment of the sordarin-binding cavity changes significantly from one species to another depending on the species specific substitutions within the cavity. Moreover, eEF2 binding to ribosome aggravates the effects of these substitutions. Thus, this study, while shedding light on the molecular mechanism underpinning the selective inhibitory effects of sordarin, will also be a helpful guide for future studies aiming at developing novel antifungal drugs with broader spectrum of activity.

Keywords Protein synthesis · tRNA translocation · Elongation factor-2 · Drug-binding pocket · Micro-environment · Structural analysis

Introduction

Synthesis of proteins by linking individual amino acids is a fundamental process in the cells of all living organisms. Proteins are synthesized by ribosomes, mega-dalton RNA–protein machines, that use cognate transfer RNAs (tRNAs) to translate the message encoded in the messenger RNA (mRNA) in all living cells [1]. In the course of protein synthesis, tRNA occupies successively the universally conserved A (aminoacyl), P (peptidyl), and E (exit) sites of the mRNA-programmed ribosome [2]. The elongation cycle of translation, during which a new amino acid is added to the growing polypeptide chain, is a repeating, three-step process encompassing aminoacyl-tRNA (aa-tRNA) selection, peptide bond formation, and mRNA–tRNA translocation [3]. Translocation, the final step of the elongation cycle, is a crucial step of protein synthesis catalyzed by the binding of the translocase eEF2 (EF-G in prokaryotes) and subsequent GTP hydrolysis [4]. The translocase promotes the complete translocation of the deacylated tRNA and peptidyl-tRNA into the E- and P-sites, respectively in a precise and controlled manner. In addition, the mRNA advances by one codon to allow the next codon to move into the decoding centre.

Sordarin belongs to a class of natural products with multiple functional groups readily accessible to chemical modification. The primary target of the drug is eEF2 [5, 6] and it is known that, although eEF2 by itself can bind sordarin, presence of ribosome is important for high affinity binding [5–10]. Until recently it was believed that

Electronic supplementary material The online version of this article (doi:10.1007/s10822-013-9636-8) contains supplementary material, which is available to authorized users.

B. Chakraborty · R. Mukherjee · J. Sengupta (✉)
Structural Biology and Bio-Informatics Division, Indian Institute of Chemical Biology (Council of Scientific and Industrial Research), 4, Raja S.C. Mullick Road, Kolkata 700 032, India
e-mail: jayati@iicb.res.in

sordarin stops translation only at the elongation stage by blocking translocation and ribosome-bound eEF2 being its functional target [10]. But recent studies demonstrate that sordarin also inhibits eEF2-ATP mediated ribosome splitting [11]. Thus the current view encapsulates the idea of dual inhibitory action of sordarin to impair translation.

Interestingly sordarin and its derivatives have been shown to inhibit translation specifically in yeast and certain filamentous fungi by impairing eEF2 function [5, 12–14] while failing to do the same even in some other fungi and also in human [15] in spite of the fact that all the fungal as well as the human eEF2s share reasonable sequence identity. A biochemical study [15] elucidated that a stretch of eight residues (517–524 in yeast) at the entrance of the sordarin-binding cavity determines the sordarin binding specificity for different eEF2s and that stretch (Fig. 1d) has been termed as "sordarin specificity region" (SSR). So it seems quite obvious that the binding cavity for sordarin in eEF2 plays a vital role in determining this specificity.

Knowing all these facts we asked the question how actually the different substitutions in the SSR (along with certain other cavity residues apart from those within the SSR) affect the sordarin-binding cavity of eEF2s of different fungal species and human so as to make them respond so much differently to sordarin and whether the presence of ribosome plays any role to account for such a remarkable specificity.

To this end, we have analyzed the sordarin-bound states of yeast eEF2 in both isolated (not bound to ribosome) and ribosome-bound forms and also the same for eight other fungal eEF2s. Along with the fungal species we have also analyzed the sordarin-binding cavity of the human eEF2. Our analysis mainly dealt with investigation of the physical as well as chemical compatibilities of the drug molecule with the drug-binding pocket of different eEF2 structures in order to decipher the feasibility of the drug binding inside the cavity of different eEF2s.

Differential sensitivity of various eEF2s towards the drug as revealed by our study elucidated that the local environment of the drug-binding cavity indeed plays the key role in determining sordarin selectivity. Thus, this study has furnished structural insights into the mechanism of species-specific inhibition of protein synthesis by sordarin.

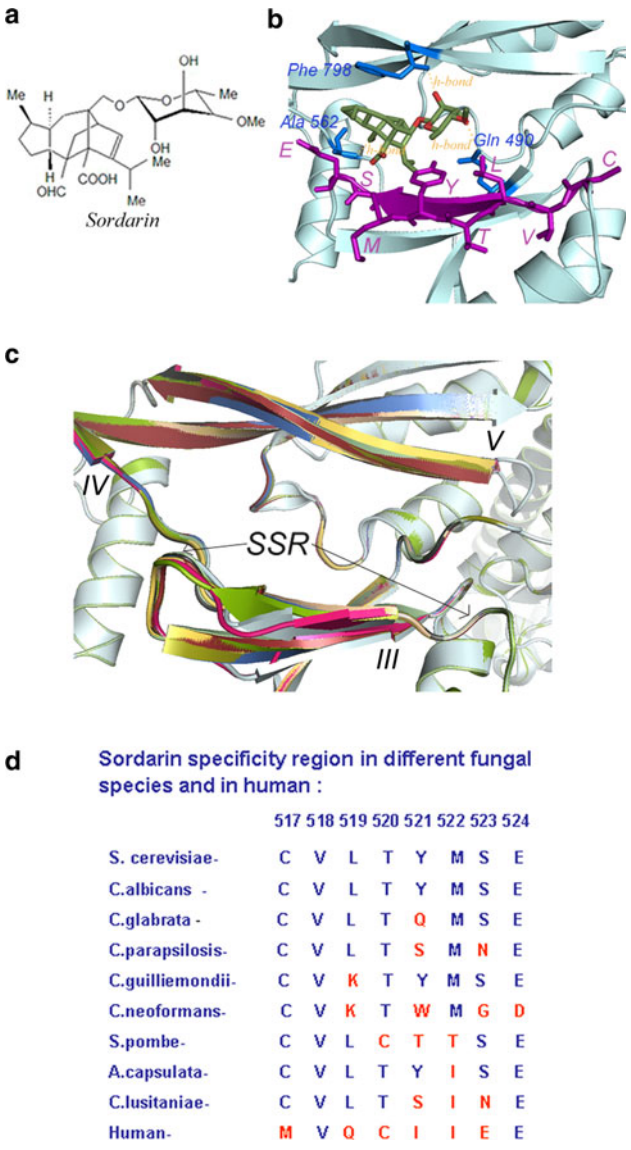

Fig. 1 Sordarin and 'Sordarin Specificity Region' in eEF2. **a** Chemical structure of the sordarin molecule. **b** Sordarin within its binding cavity of yeast eEF2 (shown in *cyan*). The three yeast eEF2 residues, Gln490, Ala562 and Phe798 forming hydrogen bonds with sordarin (according to the crystal structure), are shown in blue sticks and the SSR residues are displayed in violet sticks. **c** A close-up view of the sordarin-binding cavity of different fungal eEF2s overlaid onto one another. Yeast eEF2 is shown in cyan blue the other eEF2s are shown in different colours. It is clearly seen that while rest of the eEF2 structures are superimposed very nicely, the SSR regions of different species deviate significantly with respect to the SSR of yeast eEF2. **d** The amino acid sequences in the SSR across different fungal species and human [15] are aligned. The mutated residues with respect to yeast are shown in red. It is seen that most of the SSR residues in human eEF2 are mutated with respect to yeast eEF2. In contrast, for fungal eEF2s, varied substitutions at the position 521 are present

Methods

Homology modelling of the eEF2 structures of different species

We have generated two sets of eEF2 models for all the fungal species that we have selected for this study, representing isolated and ribosome-bound forms of the protein by exploiting high sequence homology (Supplementary Fig. 1). The templates used for homology

modelling were: (i) a crystal structure of sordarin-bound yeast eEF2 (RCSB PDB code 1N0U) for isolated form, and (ii) a model structure of sordarin-bound yeast eEF2 (RCSB PDB code 2P8Y) in complex with fungal ribosome for ribosome-bound form. Since there is no structural information available on eEF2-bound human ribosome, the ribosome-bound eEF2 model for human was excluded and only the model representing isolated eEF2 was generated. Sequences of the eEF2s of eight fungal species which are reported to interact differently with sordarin and also that of human eEF2 were retrieved from ExPASY UniProt server (http://www.uniprot.org/). Protein models for the target sequences were constructed using the homology module within InsightII (Accelrys, San Diego, CA) implemented on a Silicon Graphics workstation. Sequence alignment was refined manually to reduce to the minimum gaps which were not allowed inside the structural elements. Each model was also opportunely minimized using the Discover3 module within InsightII (Accelrys, San Diego, CA). The high sequence identity and sequence similarity (Supplementary Fig. 1) justify the suitability of the sordarin-bound yeast eEF2 structures (1N0U and 2P8Y) as the template for modelling the 3D structures of the eEF2s of all the different species in consideration. The resulting model structures were verified using PROCHECK [16] (PDBsum server http://www.ebi.ac.uk/pdbsum/).

Additionally we have also generated some mutant eEF2 models by computationally substituting residues using Accelrys Discovery Studio and then the drug was docked within the cavity using flexible docking procedures (discussed below).

Preparation and optimization of the model 2P8Y

In absence of any high-resolution ribosome-bound eEF2 structure, we have used a quasi-atomic model of sordarin-bound yeast eEF2 (RCSB PDB code 2P8Y) in complex with ribosome. Since 2P8Y is a model obtained by fitting eEF2 crystal coordinates into a low-resolution cryo-EM map of eEF2-bound 80S ribosome stalled by sordarin (80S.eEF2.GDP-sordarin complex [10]) we had to carry out meticulous optimization of the model before using it for our analysis. 2P8Y was previously constructed by fitting the eEF2 crystal structure as two individual rigid bodies: domains G′, I and II making up one rigid body, while domains III, IV and V forming the second rigid one [10] because the relative orientation of the domains G′-I-II and III-IV-V of eEF2 changes in the ribosome-bound form. Therefore, in the model, the intra-domain structures and the inter-domain contacts remained virtually the same as they are in the crystal structure except the conformation of the linker region between domains II and III. Although this region does not belong in the cavity forming region, we have constructed the missing link between the domain II and III. In order to do that we have aligned the domains III (containing the stretch of amino acids linking domain II and III) -IV-V of the crystal structure with the model, taken the linker sequence from the crystal structure, recreated the peptide bonds in 2P8Y model and then minimized the complete model structure. Furthermore, we subjected the minimized 2P8Y model to a rigorous two step flexible affinity docking (procedure described in detail in following section) to get a much realistic cavity structure and ligand position. This optimized model was finally considered as the structure representing the ribosome-bound state of eEF2-sordarin complex for yeast (*S. cerevisiae*) and was used as the template for generating homology models representing the ribosome-bound forms of eEF2-sordarin complex for different fungal species. In addition, we have also analyzed the eEF2 model (2P8Z) fitted into the cryo-EM map of the 80S.eEF2.GDPNP.sordarin complex (EMD-1345) in the similar manner as described above.

Docking of the ligand

The position of the drug inside its binding cavity was optimized using rigorous docking procedures. Preliminary docking was done using Z-DOCK (http://zdock.umassmed.edu/) [17] (rigid body docking), then the binding was fine-tuned by applying flexible docking algorithm as implemented in the Affinity module in InsightII. Affinity is a suite of programs for automatically docking a ligand to a receptor by a combination of Monte Carlo minimization and Simulated Annealing procedure (Affinity user guide. San Diego, USA: Accelrys Inc.; 1999). The residues of the protein present at <5 Å from the 'pre-docked' ligand was defined to be the binding subset and were kept flexible. The bulk of the host, defined as residues not in the binding subset, was kept rigid during the docking process. The 10 starting structures for the protein–ligand complexes (eEF2-sordarin) for various fungal species were generated by Monte Carlo minimizations. The parameters of minimization were 100 minimization steps performed by the Quartic_vdw_no_Coul method as a non-bond summation procedure, with the convergence of 1×10^{-6} kcal/mol used as the energy test and 1 Å used as the RMSD tolerance threshold. Simulated annealing was then applied for each respective selected complex with 50 stages of 100 fs, the initial and final temperatures being 500 and 300 K, respectively. Extensive affinity docking was performed by changing various docking parameters.

The resulting set of complexes obtained had the ligand bound to the cavity in various poses. Since the proteins are highly homologous, the drug was expected to be positioned very similarly in the cavities for all the species. As expected, all the top-ranked poses in each case were indeed

quite similar to the ligand orientation observed in the crystal structure (RMSD not more than 2 Å). In order to select the final ligand-bound structure in each case, all the top-ranked ligand poses were evaluated to find the least deviated pose as compared to the yeast structures (1N0U for isolated form and optimized 2P8Y for ribosome-bound form) based on heavy-atom RMSD (calculated using the ANALYSIS module of InsightII program) values. RMSD values of the final structures in each case was <1 Å.

Analysis of the ligand-bound cryo-EM map

We analyzed the cryo-EM map (EMDB-1344) of a complex of 80S ribosome (*T. lanuginosus*), eEF2 (*S. cerevisiae*) (in GDP state) and sordarin [10]. SPIDER [18] was used for the computational separation of the cryo-EM reconstruction into densities corresponding to individual ribosomal subunits or eEF2. Isolation of the ligand mass from the cryo-EM map was performed according to a segmentation procedure available in SPIDER. In brief, the 80S ribosome was first masked out from the map of the complex. Next, selection of the mass of interest from the remaining masses was performed using a clustering procedure (http://www.wadsworth.org/spider_doc/spider/docs/techs/isolate.html).

Analysis of the compatibility between the cavity and the ligand

The program CASTp (http://sts.bioengr.uic.edu/castp/calculation.php) [19] was used for preliminary assessment of the binding cavities inside the eEF2 structures. In order to study variations in the sordarin-binding cavity among different eEF2s, we have generated the 'positive casts' of the cavities of both the template eEF2 structures as well as for all the models built against both the templates. We created the density map for each of the eEF2 coordinates and inverted the density maps using thresholds calculated on the basis of molecular volume estimates so as to get the exact densities for the cavities. The map parameters of EMDB-1344 were used for generating the density maps from pdbs in order to keep consistency. We have isolated one continuous mass corresponding to the sordarin-binding cavity from the resulting inverse map using clustering procedure available in SPIDER. The 'positive cast' of the sordarin-binding cavity, therefore, represents the 3D shape and size of the cavity interior. Thresholds for all displayed positive and inverted density maps were chosen based on molecular volume estimates as described in a previous study (see [20]).

To quantify how well the drug is physically fitted within the different cavities, a simulated map was generated from the fitted atomic structure of the drug molecule with the same target resolution as the EM map. The cross-correlation coefficient (Pearson's correlation coefficient) [21] between the simulated (drug molecule) and the experimental ('positive cast') maps can be used as a measure of similarity between them. All cross-correlation coefficients were computed considering only voxels inside the molecular envelope of the simulated map ("local correlation") [22]. The cross-correlation coefficient (cc c) between the 'positive cast' and the sordarin density for each case was calculated using SPIDER [18].

Analysis of ligand–protein contacts

The analysis of ligand–protein contacts was done using a server named LPC/CSU (http://ligin.weizmann.ac.il/cgi-bin/lpccsu/LpcCsu.cgi) within a suite named SPACE [23]. It gives a normalized complementarity (NC) value for each protein–ligand complex based upon the intermolecular atomic contacts between them. This parameter provides estimation for the possibility of the ligand binding to its receptor.

Now, the equation solved is:

$$NC = CF/MC$$

(where CF is the complementarity function and MC is the maximum complementarity).

Again, the complementarity function is defined as:

$$CF = S_l - S_i - E$$

(where S_l is the sum of all surface areas of legitimate atomic contacts between ligand and receptor, S_i is the sum of all surface areas of illegitimate atomic contacts, and E is a repulsion term).

So, finally NC depends upon the surface area of the ligand engaged in contacts contributing in its binding (legitimate atomic contacts) and the surface area of contacts not contributing in its binding (illegitimate atomic contacts). Again, legitimacy depends on the hydrophobic-hydrophilic properties of the contacting atoms.

Estimation of surface area of the protein-bound ligand and the electrostatic environment within the cavity

Analysis of accessible surface area (ASA) and Coulomb potential map of the ligand were done using SPACE and Chimera [26]. ASA provides a measure about how well the drug in buried inside the binding pocket. Electrostatic surface potential maps of the proteins, based on the Poisson Boltzmann (PB) model that constitutes the fundamental equation of electrostatics, were generated using the Adaptive Poisson Boltzmann Solver (APBS) software [24] available with the PyMol interface. Colour code units are in ±10 kT/e. Visualization and preparation of illustrations

were done using PyMol (DeLano Scientific), VMD [25], and Chimera [26].

The 'deterministic parameters' and binding likeliness of sordarin

All the parameters described above were used to quantify our analysis. We have characterized all the cavities and predicted the binding likeliness of the drug based on these parameters collectively. While the cross-correlation coefficient (cc c) gives an estimate whether the shape and size of the available space within the cavity is appropriate to accommodate the drug or not, the complementarity value suggests how the interaction between the cavity residues influence drug binding. On the other hand the ASA gives an idea how well the drug is buried inside the cavity (well-fitted). Briefly, the above mentioned parameters collectively provide an estimate of the compatibility of the drug and the drug-binding pocket (both physically and chemically) from species to species in a comparative manner.

Since the sordarin sensitivity of yeast has already been established by different experimental studies, the values of these parameters obtained for yeast eEF2 in both isolated and ribosome-bound forms were considered as those indicating sensitivity for sordarin in the two respective forms. Coming to the eEF2s of other species, a species under consideration have been considered to be 'sordarin sensitive' only if values of all the three parameters of that species fall in the same range as those of yeast. On the other hand, the species with the value of even one parameter drastically deteriorated or two or more poor values are considered as 'insensitive'. In other words, the values of all the three parameters have been collectively considered as a function.

It must be noted here that the absolute value obtained for each of the parameters doesn't have much significance. The values should only be considered as estimates for comparative analysis.

Results and discussion

Structural basis for the recognition of sordarin by eEF2

As a first step in understanding specific interactions between the drug and the drug-binding cavity, and also the physical compatibility between them, we have analyzed the available X-ray crystal structure of the sordarin-bound yeast eEF2 complex (eEF2-sor) closely.

The crystal structure (pdb code 1N0U) of eEF2-sor showed [27] that the sordarin molecule (Fig. 1a) binds in a pocket between domains III, IV and V (Fig. 1b, c). It shows that there is only one possible entry for the cavity because domain IV effectively blocks the other side.

The stretch of amino acids identified as sordarin specific region (SSR) belongs to domain III of eEF2 that makes the lower part of the entrance of the drug-binding cavity. Juxtaposition of different model eEF2 structures with the yeast eEF2 crystal structure revealed that, while rest of the structure superimposes nicely, conformations of the stretch of amino acids, identified as 'SSR' [15], appears significantly different (Fig. 1c).

The crystal structure has also identified [27] some functionally relevant amino acid residues like Gln490, Ala562 and Phe798 which are directly involved in the formation of hydrogen bonds (Fig. 1b) with sordarin. Additionally, extensive van der Waals interactions are also reported between sordarin and aromatic or aliphatic side chains of eEF2. The crystal structure also showed three water molecules in the cavity mediating contacts between sordarin and the protein. We have omitted the water molecules for our calculations because, for the modelled structures, placement of the water molecules would not be very reliable.

Preliminary CASTp analysis readily identified the cavity between domains III, IV and V of the eEF2 crystal structure (Fig. 2a). The 'positive cast' created for the yeast (*S. cerevisiae*) eEF2 cavity matches well with the curvature of the inner surface of the cavity identified by CASTp (Fig. 2b) suggesting that the 'positive cast' truly represents the 3-dimentional (3D) physical features of the cavity interior. Visualization of the drug molecule inside the 'positive cast' clearly shows that the drug is fully embedded inside the cavity for the *S. cerevisiae* eEF2 (Fig. 2c).

Sordarin-binding cavity in elongation factors across species

We have investigated how the drug-binding cavity of human eEF2 has been modulated by nature so as to make it completely insensitive to sordarin. In human eEF2 sequence, despite considerable overall sequence identity and similarity with yeast (Swissprot: Human, P13639; *S. cerevisiae*, P32324; yeast vs. human eEF2: more than 60 % identity, more than 70 % similarity), almost all the residues (6 out of 8) in the SSR are mutated to different amino acids (Fig. 1d). We suspected that such a large scale mutation within a short stretch of amino acids might cause a drastic change in the overall hydropathy of the SSR. But to our surprise we found the overall hydropathy indexes [28] for the SSR of yeast and human eEF2 to be quite similar ($\sim$6.5, human one being slightly more hydrophobic). But interestingly, the patterns of hydrophobicity/hydrophilicity are distinctly different (Fig. 3a). The region that is hydrophobic in the SSR of yeast eEF2 is hydrophilic in corresponding human eEF2 sequence and vice versa suggesting that if the SSR sequence in yeast eEF2 favors sordarin

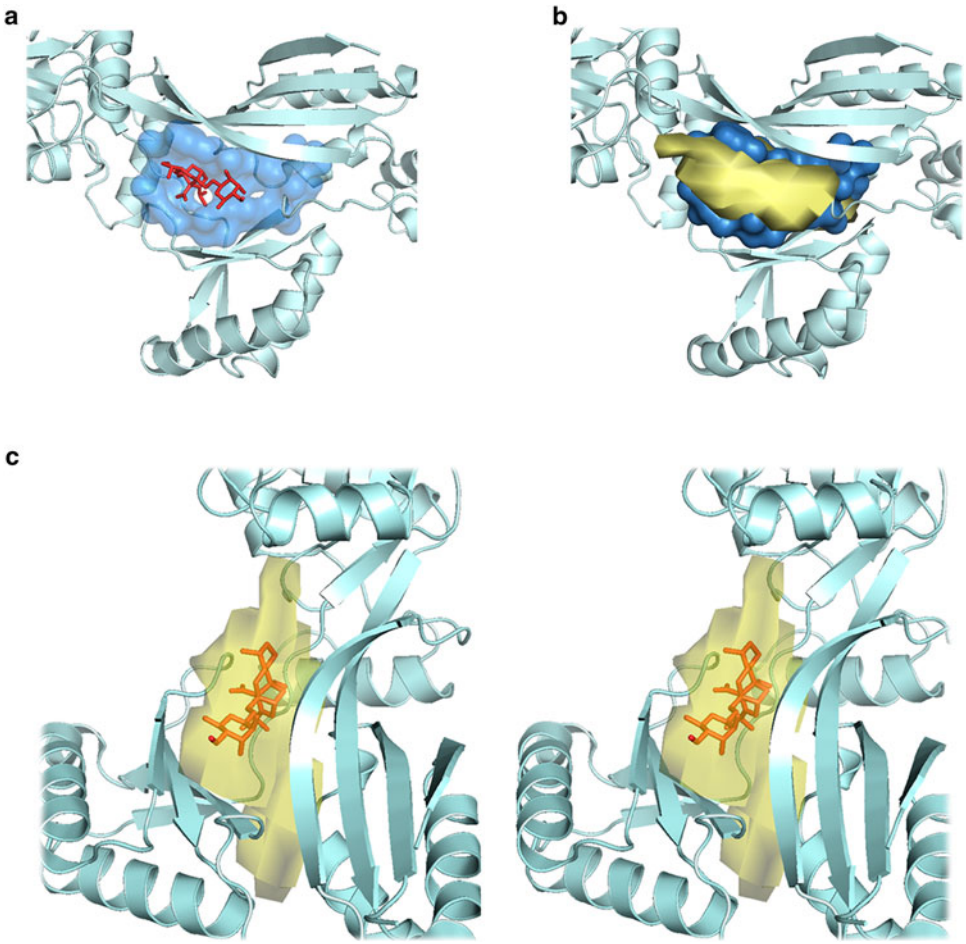

Fig. 2 Overview of the sordarin-binding pocket in yeast (*S. cerevisiae*) eEF2. **a** Close-up view of the outline of sordarin-binding cavity (*blue*) in yeast eEF2 as obtained by CASTp (with sordarin (*red*)) which traces the internal physical features of the cavity. **b** The 'positive cast' (*yellow*) computed for the sordarin-binding cavity (representing the cavity in terms of density) smugly fitted within the CASTp obtained cavity curvature (*blue*) assuring that the 'positive cast' actually accounts for the internal features of the cavity. **c** Close-up view (in stereo) of sordarin bound yeast eEF2 (*cyan*) with the 'positive cast' (*semitransparent yellow*) of the sordarin-binding cavity showing that the drug (*red*) is fully accommodated within the cavity of *S. cerevisiae* eEF2

binding the same in human eEF2 is expected to be unfavorable.

Interestingly, we found that apart from the mutations within the SSR, known to be responsible for binding specificity of sordarin [15], some other mutations in the human eEF2 cavity also play vital role in making human eEF2 insensitive to sordarin. Among those residues Gln490 and Ala562 in *S. cerevisiae* (Fig. 3b) which form hydrogen bond with sordarin in *S. cerevisiae* [27] are mutated in human to Arg506 and Ser578 respectively (Fig. 3c). While both the mutations are involved in minimizing the favorable contacts like hydrogen bonds and generating unfavorable contacts with sordarin (Supplementary Table 1), the mutation from Gln490 to Arg506 also likely affects the electrostatic interaction with sordarin due to its positive charge (Supplementary Fig. 2). Another mutated residue Tyr745 (Phe729 in *S. cerevisiae*) in human cavity comes very close to residue Arg506 (Fig. 3c) unlike their counterparts in *S. cerevisiae* cavity (Fig. 3b) and it is evident that together they squeeze the drug-binding cavity in human eEF2 (Fig. 3c). Yet another mutated residue Lys619 (Asn603 in *S. cerevisiae*) is positioned at the entrance of the cavity (Fig. 3c) and is sure to cause hindrance in the drug entry by virtue of its bulky size and positive charge compared to its yeast counterpart (see also Supplementary Fig. 2).

The lower complementarity value for human eEF2 compared to that of *S. cerevisiae* (Table 1) indicates that the drug-binding cavity of human eEF2 is much less chemically compatible for sordarin binding as compared to *S. cerevisiae* eEF2. A much lower cross-correlation coefficient (cc c) is also observed for sordarin inside the human eEF2 pocket as compared to that of sordarin within the cavity of *S. cerevisiae* eEF2 (Table 1), indicating the human eEF2 cavity to be

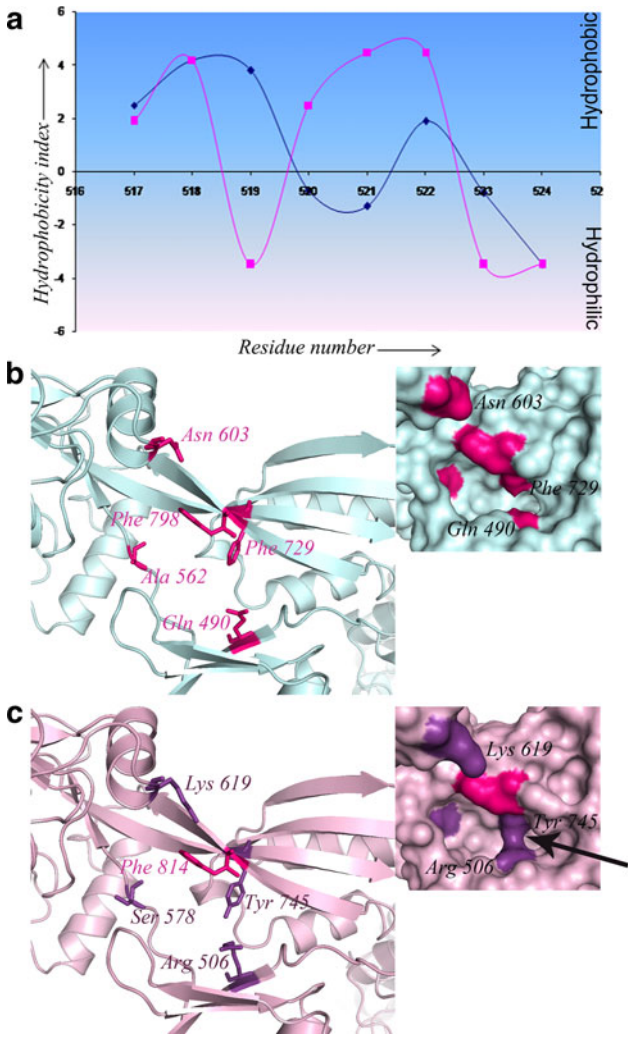

Fig. 3 Comparison between the sordarin-binding cavity of yeast and human eEF2. **a** A plot showing the relative hydrophobic nature of the SSR residues of yeast versus human eEF2 obtained by plotting Hydropathy index (Kyte-doolittle method, [28]) against the SSR residues. It is clear that the nature of hydrophobicity/hydrophylicity of SSR stretch is inverted for human when compared to yeast. **b** Close-up view of the yeast eEF2 cavity showing important residues (*pink*) which take part in interactions with sordarin (according to the X-ray structure) in sticks. In the inset the cavity is shown in surface representation with the same residues coloured in *pink*. **c** The human eEF2 cavity with the corresponding residues shown in sticks with the cavity shown in surface in the inset. Among these residues which are mutated in human are coloured in *violet*. In the inset, the piller-like structure in the human cavity formed by the two mutated residues (Arg506 and Tyr745, corresponding to Gln490 and Phe729 respectively in yeast) imposing obstruction in the cavity is indicated by an arrow. Another mutation Lys619 (corresponding to Asn603 in yeast) at the entrance of the cavity is also shown. All these changes make the cavity drastically different for human as compared to yeast

physically incompatible for drug binding as well. The solvent ASA of the drug within the cavity is also higher in human eEF2 compared to that in case of *S. cerevisiae* eEF2 (Table 1) suggesting that the drug is not fully encompassed by the cavity of human eEF2.

All these findings clearly suggest that in case of human eEF2, the mutations within the SSR as well as the other amino acid substitutions (unique for human eEF2) at vital positions discussed above collectively make its drug-binding cavity drastically different from its fungal counterparts so as to rule out any possibility of binding or even the entry of the drug.

Sordarin-binding cavity in elongation factors of different fungi

In an effort to understand, in molecular terms, the binding selectivity of sordarin towards isolated eEF2 (eEF2 not bound to ribosome is termed as isolated eEF2) across different fungal species we have analyzed the eEF2 models (in complex with sordarin) of several fungi namely, *Candida albicans* (Swissprot: O13430), *Candida glabrata* (Q6FYA7), *Candida gulliermondii* (A5DI11), *Candida parapsilosis* (Q9P4R9), *Candida lusitanae* (C4YCF8), *Cryptococcus neoformans* (Q5KHJ9), *Ajellomyces capsulata* (C0NSN4), *Schizosaccharomyces pombe* (O14460) along with the crystal structure of *S. cerevisiae* eEF2 bound to sordarin (1N0U). Sequence alignment of the eEF2s of different fungal species (Supplementary Fig. 1) readily shows high sequence similarity (sequence identity more than 80 %, and similarity more than 90 %) among them.

Upon quantification it was revealed that the complementarity (the determinant of chemical compatibility) between the drug and the drug-binding cavity almost remains the same for all the species with exception for *C. lusitanae*. However, upon considering all the 'deterministic parameters' together, it appeared that while *C. albicans, C. guilliermondii, and A. capsulata* shows similar degree of sensitivity for sordarin as *S. cerevisiae*; *C. glabrata, C. parapsilosis C. neoformans*, *S. pombe* and *C. lusitanae* shows varying degrees of insensitivity for the drug (Table 1). Thus, physical compatibility apparently plays a more prominent role compared to chemical compatibility in governing sordarin's selectivity for binding to the cavity of various fungal eEF2s. We have assessed physical compatibility by the cross correlation coefficient (cc c) between the 'positive cast' of the cavity and the ligand, along with the ASA of the ligand following binding to the receptor. All the cavity residues collectively contribute to form the internal shape and size of the cavity ('positive cast'). Therefore, the effect of overall differences in cavity residues including SSR is reflected in the cc c values.

According to available biochemical results [5, 14, 15, 29] it is known that sordarin and its glycone-substituted derivatives inhibit growth of different fungal species such as *C. albicans*, *C. tropicalis* and *C. neoformans*, *C. glabrata* at

Table 1 Parameters [Complementary (Compl.), Cross-correlation coefficient (cc c) and accessible surface area (ASA)] used to evaluate the binding affinity of sordarin to eEF2 both in isolated and ribosome-bound forms across different fungal species

eEF2 versus sordarin	Isolated eEF2				Ribosome-bound eEF2			
	Compl.	cc c	ASA (Å^2)	Sensitivity	Compl.	cc c	ASA (Å^2)	Change in sensitivity
Saccharomyces cerevisiae (s)[15]	0.55	0.68	~164	s	0.54	0.66	~139	Increase
C. albicans(s)[14,15]	0.62	0.68	~160	s	0.60	0.64	~151	Similar
C. guilliermondii (ps)[15]	0.66	0.63	~168	s	0.58	0.61	~165	Similar
Ajellomyces capsulata	0.56	0.72	~172	s	0.59	0.68	~147	Increase
C. neoformans (ps)[15]	0.59	0.58	~182	is	0.63	0.72	~140	Increase
C. glabrata (ps)[15]	0.52	0.43	~166	is	0.47	0.61	~158	Increase
C. parapsilosis (is)[14,15]	0.56	0.56	~190	is	0.42	0.48	~182	Decrease
S. pombe	0.51	0.49	~180	is	0.50	0.63	~176	Increase
Candida lusitaniae (is)[15]	0.45	0.51	~198	is	0.32	0.61	~145	Similar
Human *(is)*[15]	0.44	0.54	~177	is	–	–	–	–
S. cerevisiae (2P8Z)	–	–	–	–	0.50	0.55	~182	–
C. glabrata (^{Gln}***521***$_{Tyr}$)[a]	0.52	0.57	~160	s	–	–	–	–
C. glabrata (^{Gln}***521***$_{Trp}$)[b]	0.52	0.65	~172	s	–	–	–	–
S. cerevisiae (^{Tyr}***521***$_{Trp}$)[c]	0.64	0.65	~156	s	–	–	–	–

The different fungal species are arranged in decreasing order of degree of sordarin sensitivity shown by them in isolated form. The values of the parameters for human eEF2 in isolated form have also been provided. The table also shows the same parameters for the mutated eEF2s in isolated form. ["s" stand for "sensitive", and "is" stands for "insensitive"]

[a] The amino acid at position 521 is mutated from *Glutamine (Gln)* to *Tyrosine (Tyr)*

[b] The amino acid at position 521 is mutated from *Glutamine (Gln)* to *Tryptophan (Trp)*

[c] The amino acid at position 521 is mutated from *Tyrosine (Tyr)* to *Tryptophan (Trp)*

different concentrations while other species including *C. parapsilosis, C. lusitaniae* and *C. krusei* are insensitive to high levels of these compounds (Table 1). However, there exists some contradiction between the experimental studies [14, 15, 29] regarding the level of sordarin sensitivity or resistance for different fungal species. Sensitivity predicted from our analysis is consistent with the experimentally judged sensitivity of sordarin (Table 1).

It has been shown that sordarin competes with ATP/ADP for eEF2 binding in solution indicating that the binding sites of the two on eEF2 might be overlapping [30]. Intriguingly, sordarin does not seem to inhibit ATP binding to the complex of the 80S ribosome and eEF2 [11]. These results contextualize sordarin's interaction with eEF2 in isolated form. A plausible pathway is that sordarin inhibits eEF2-ATP dependent ribosome splitting by binding to eEF2 in the isolated form and thus blocking ATP binding to eEF2, and the differential sensitivity of sordarin towards various fungal eEF2 in isolated form may have important implication in determining the efficacy of eEF2.ATP-mediated ribosome splitting in different fungi.

Importance of residue at 521 in determining sordarin sensitivity

It is conceivable that the overall sequence and 3D structure being the same the local conformation of the drug-binding cavity plays a crucial role in binding specificity of the drug. According to an earlier mutational study [15], three amino acid residues within the SSR (Fig. 1d) at positions 521, 523, 524 (sequence numbering as in *S. cerevisiae*) particularly determine the specificity of sordarin binding. Of the three residues while the position 524 was found to be either conserved or substituted by similar residue for the species in consideration, most of the polymorphisms are seen at positions 521 and 523 (Fig. 1d). Of the two positions (521 and 523), we found 521 to be more fascinating since varied substitutions take place at this position in different species (see Fig. 1d).

It is seen that, in *S. cerevisiae* eEF2, Tyr521 makes extensive favorable contacts with the drug which is reflected in the total favorable surface area offered by this residue (Table 2; Fig. 4a). However, the hydroxyl group (OH) of Tyr residue is involved in unfavorable contacts with the drug (Table 2). In *C. glabrata* and *C. parapsilosis* where Tyr has been replaced by Gln (Fig. 4c) and Ser (Fig. 4d) respectively, we observed a drastic reduction in the favorable surface area offered by these two altered residues (Table 2). Interestingly, in case of *C. neoformans* (Fig. 4b) where Tyr521 has been substituted by Trp, we found the favorable surface area offered by Trp to be even more than that of Tyr (Table 2). These observations led us to speculate that substitutions at the position 521 can both stabilize and destabilize drug binding depending on the

nature of substitution taking place and thus can play a critical role in dictating the degree of sordarin sensitivity or resistance.

In order to check this idea we did some mutational analyses. First, we mutated the Gln521 in *C. glabrata* to Tyr so as to make the SSR of *C. glabrata* same as that of *S. cerevisiae*. It was found that the cross-correlation value (indicating physical compatibility) increases considerably keeping the complementarity value (indicating chemical compatibility) unchanged with also a slight decrease in the accessible surface area (ASA) value (Table 1). Further, the favorable surface area offered by the mutated Tyr residue in *C. glabrata* becomes the same as that offered by the Tyr residue in *S. cerevisiae* (Table 2). Notably, in this case also it was observed that the negative effect of the hydroxyl group (OH) of Tyr residue persists (Table 2). All these parameters together suggest improvement in binding probability of sordarin in presence of Tyr in place of Gln at position 521 within the cavity of C. *glabrata*. Mutation of Gln521 to Trp showed an increase in the cross-correlation value (Table 1) even more. Interestingly, substitution of Tyr521 by Trp indicated positive effect on sordarin binding for *S. cerevisiae* eEF2 also (Table 2). Based on these observations it can be concluded that aromatic residue at 521 (particularly Trp) makes the cavity more favorable for sordarin binding.

It may be noted here that although Trp at 521 for *C. neoformans* offers considerable favorable surface of contact, overall binding likeliness for *C. neoformans* eEF2 was inferred low (Table 1) indicating that other modifications in the cavity residues (Supplementary Fig. 1) counteract the positive effect of Trp.

Ribosome-bound conformation of eEF2 and sordarin binding

It has been suggested by previous studies that ribosome-bound eEF2 is the primary functional target of sordarin [9, 10]. One of the structural studies explored the full translocation process by trapping eEF2 on the ribosome at different intermediate stages of tRNA translocation [10]. Four cryo-EM maps (EMD-1342, EMD-1343, EMD-1344, and EMD-1345) have been obtained from this study along with four corresponding fitted eEF2 models (pdb codes: 2P8W, 2P8X, 2P8Y and 2P8Z respectively).

It was shown that sordarin does not inhibit GTP hydrolysis on eEF2, and the studies suggested that sordarin prevents further conformational change in eEF2 following GTP hydrolysis that facilitates the release of the factor [8–10] implying that, irrespective of which state of eEF2 sordarin binds to, the ribosome-bound eEF2-GDP state is actually the functional target of the drug. Hence, first we have analyzed the map corresponding to the 80S.eEF2.GDP.sordarin complex (EMDB-1344) and the eEF2 model associated with this state (2P8Y). Density attributed to sordarin can be resolved in the cryo-EM map (EMD-1344; Fig. 5a), and the ligand appears at the location known from the X-ray map of sordarin-bound eEF2 (Fig. 5b). We have segmented out the eEF2-sordarin density from the map (Fig. 5a). The docked 'quasi-atomic model' [31] associated with this structure (2P8Y) clearly shows how well (with a cross correlation value $\sim$0.9) the eEF2-sordarin model corresponds to the eEF2-sordarin density isolated from the map (Fig. 5b) justifying the feasibility of using this model as the template structure.

It is observed that, if only the domains III, IV and V are overlaid (Fig. 6a), relative orientation of the domains are not drastically different in isolated and ribosome-bound forms of eEF2 except a rotation in domain III occurs in ribosome-bound form which is likely promoted by the 'ratchet-like movement' (large-scale conformational change induced by the binding of EF-G/eEF2) [9, 32] of the small subunit upon eEF2 binding.

In the ribosome-bound conformation the picture in terms of the deterministic parameters changes considerably.

Table 2 Contribution of various residues at position 521 on sordarin binding sensitivity

Residue 521 versus sordarin contacts	Surface area of interaction with sordarin (A^2)		No. of favorable contacts		No. of unfavorable contacts	
	Surface area of favorable interaction (A^2)	Surface area of unfavorable interaction (A^2)	Hydrophobic interaction	Hydrogen bond	Acceptor-acceptor	Hydrophilic-hydrophobic
Tyr *S. cerevisiae*	59.8	24.9	7	Nil	Nil	2 (OH)[a]
Trp *C. neoformans*	90	0.2	6	Nil	Nil	1
Gln *C. glabrata*	31.5	14.4	3	1	Nil	3
Ser *C. parapsilosis*	11.9	4	1	2	Nil	1
$^{Gln}521_{Tyr}$ *C. glabrata*	59.6	22.4	4	1	Nil	1(OH)[a]
$^{Gln}521_{Trp}$ *C. glabrata*	91.1	0.9	6	Nil	Nil	1
$^{Tyr}521_{Trp}$ *S. cerevisiae*	87.5	0.2	8	1	Nil	1

Mutation to aromatic residue (Tyr/Trp) elicits positive effects

[a] Hydroxyl (OH) group of Tyr residue

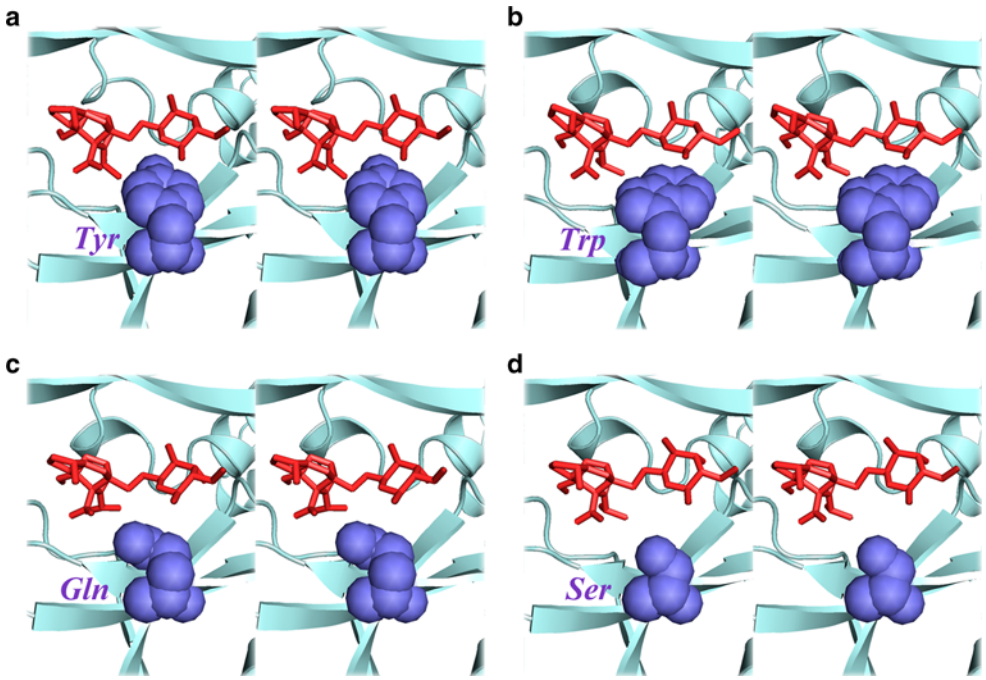

Fig. 4 Structural significance of the residue 521 in determining sordarin binding specificity. Stereo-view of sordarin (shown in *red sticks*) bound to eEF2 (*cyan*) of different species with different substitutions at position 521 (yeast numbering). **a** In yeast Tyr 521 comes very close to the ring structure of sordarin and seems to be involved in a stacking interaction. **b** In *Cryptococcus neoformans*, Trp at the same position also provides similar surface for interactions as seen in yeast. **c** In *C. glabrata* substitution of residue 521 by Gln reduces the proximity of the residue from the drug and thus reducing the possibility of any kind of favorable interaction with the drug. **d** Substitution by Ser in *C. parapsilosis* reduces the proximity of the residue from the drug even more without keeping any possibility of interacting with the drug

In case of the *S. cerevisiae* eEF2, while the complementarity and the cross correlation coefficient (cc c) values remained almost the same, a considerable decrease in the ASA (from $\sim$164 to $\sim$139 Å^2) in ribosome-bound form is observed, suggesting that sordarin fits better in ribosome-bound eEF2 (in GDP state). Visual inspection (Fig. 6b) also corroborates the fact that the shape and size of the drug-binding cavity (assessed from the 'positive cast') changes significantly in ribosome-bound form with the drug fitted more smugly as compared to the isolated form (Fig. 2b).

Although for some species eEF2 is seen to remain sensitive or insensitive in both the forms, considering the collective trend of the 'deterministic parameters' (Table 1), the changes in the values indicate that the degree of sensitivity or insensitivity changes due to ribosome binding (and/or GTP hydrolysis). In other words, it appears that the sordarin-binding cavity in various fungal species with variety of substitutions essentially becomes even more different from each other in the ribosome-bound form of eEF2 in a species specific manner depending on the SSR substitutions. However, it is also noteworthy that for some species where residues in SSR are either same or not significantly different from yeast (like *C. albicans, C. guilliermondii* and *A. capsulata*), the ASA values vary considerably more from that of yeast in the ribosome-bound form than in case of the isolated form (Table 1). This may be an indication that ribosome binding mediated changes in drug binding are not only dependent on the SSR substitutions but also on the cavity as a whole (Supplementary Table 2).

In order to understand the role of the GTP hydrolysis we have further analyzed the other states of ribosome-bound eEF2 models. A comparison between the eEF2 models for ribosome-bound eEF2 conformation at GTP state, in presence and absence of sordarin (2P8X and 2P8Z respectively) does not show any visible difference (Supplementary Fig. 3A) in the drug-binding cavity indicating that sordarin binding in GTP state does not induce any significant conformational change. In contrast, when GTP and GDP states of ribosome bound eEF2, both in presence of sordarin (optimized 2P8Z and 2P8Y models respectively) were analyzed, significant conformational change in the sordarin-binding cavity, presumably induced by the GTP hydrolysis, was clearly visible (Supplementary Fig. 3B). It appears that drug-binding pocket gets more compact in sordarin-bound GDP state. This observation prompted us to suggest, in line with the previous experimental results [4], that the presence of sordarin blocks the full range of the conformational change that occurs due to GTP hydrolysis and thus inhibit the release of eEF2 from the ribosome complex.

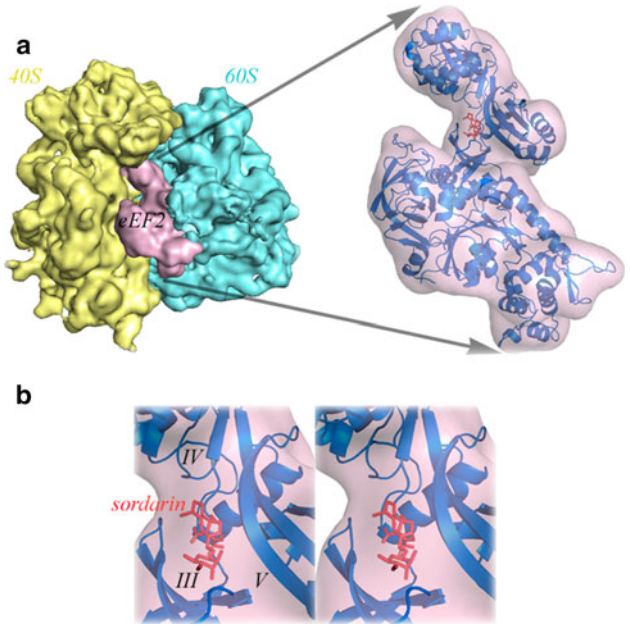

Fig. 5 Visualization of the fitted model and the eEF2 density in 80S ribosome-bound cryo-EM map. **a** Cryo-EM map of the eEF2.GDP.sordarin-bound 80S ribosome complex showing eEF2 at the intersubunit space (EMD-1344). The 40S subunit is shown in yellow and the 60S subunit is shown in *cyan blue*, and the eEF2 density is shown in pink. The inset shows the fitting (pdb code 2P8Y) of the eEF2 crystal structure (*blue ribbon*) in the density (*semitransparent pink*) attributed to the factor isolated from the cryo-EM map. The features of the density map are well-accounted for by the model coordinates. The folding of each domain in the model is essentially the same as seen in the eEF2 crystal structure (pdb code 1N0U). **b** The close-up view of the sordarin-binding region in stereo clearly shows the presence of density corresponding to sordarin molecule

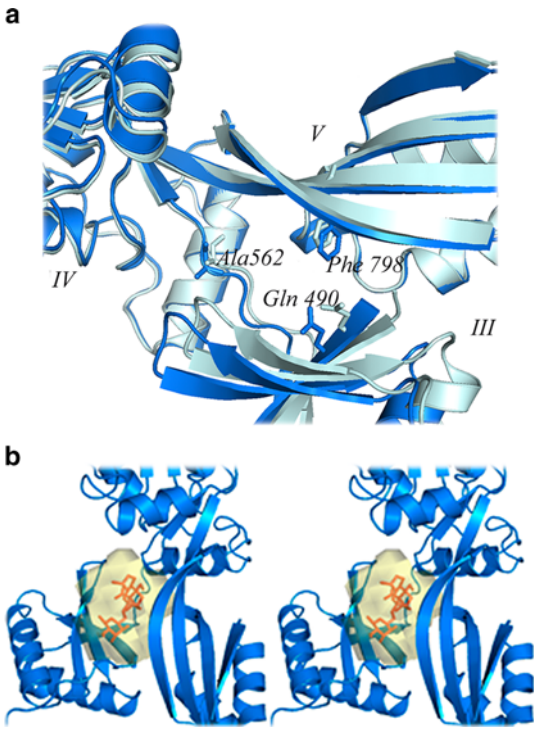

Fig. 6 Comparison between the sordarin-binding cavity of yeast eEF2 in free and ribosome-bound form. **a** Close-up view of the cavity of free eEF2 (1N0U, *cyan*) and ribosome-bound eEF2 (GDP-state; 2P8Y, *blue*) structures superimposed over one another by aligning domain III, IV and V showing overall similar orientations of the domains except domain III. The rotation of domain III makes the cavity more compact. The residues forming hydrogen bonds with sordarin are shown in sticks for both the structures. **b** Stereo-view of the cavity of ribosome-bound (GDP state) eEF2 (2P8Y) with sordarin (*red*) within the computed 'positive cast' (*semitransparent yellow*) shows that the drug is well-accommodated inside the cavity

Conclusion

In this study we have done a detailed physical and chemical characterization of the sordarin-binding cavity of eEF2 from different species. Our analysis demonstrated a clear picture of how actually the binding cavity of sordarin changes with some specific amino acid substitutions in a species specific manner so as to be resistant to the drug-binding, in spite of respectable overall sequence identity. We have provided evidence that presence of an aromatic residue at position 521(a constituent of the 'SSR') enhances sordarin-binding activity. In addition, our study has identified some substitutions within the cavity for human eEF2 (away from the 'SSR') and justified their role in determining the insensitivity for the drug. Furthermore, this study showed how conformational changes in eEF2 due to ribosome binding modulate the effects of the species specific amino acid substitutions. Our study elucidated that ribosome binding contributes significantly in determining the unique specificity of action shown by sordarin.

Based on our results, with support from previous biochemical studies mentioned earlier, we have predicted a model of the mechanism of action of sordarin in real cellular environment. According to our model sordarin targets both ribosome-bound eEF2 pool as well as free eEF2 pool depending on the growth stage of the cell and thus inhibiting either ribosome-bound eEF2 mediated tRNA translocation or free eEF2 mediated ribosome splitting and eventually causing cell death.

Further structural study on sordarin derivatives is required to identify a more effective fungicide that can target fungal eEF2s in general while being still ineffective to human eEF2. Our observation that the features of the cavity in human eEF2 is unique compared to its fungal counterparts would be helpful for setting up strategic guideline in developing new sordarin derivatives, with pan-fungal inhibitory action.

Acknowledgments The financial assistance from the CSIR-Indian Institute of Chemical Biology, Kolkata, India (BSC0113) is gratefully acknowledged. BC has been awarded senior research fellowship from Council of Scientific and Industrial Research (CSIR), Govt. of India.

Special thanks are due to Dr. N. Ghosal for extending her computer facilities to us without any reservation.

References

1. Schmeing TM, Ramakrishnan V (2009) Nature 461:1234
2. Noller HF, Yusupov MM, Yusupova GZ, Baucom A, Cate JH (2002) FEBS Lett 514:11
3. Agirrezabala X, Frank J (2009) Q Rev Biophys 42:159
4. Frank J, Gao H, Sengupta J, Gao N, Taylor DJ (2007) Proc Natl Acad Sci U S A 104:19671
5. Dominguez JM, Kelly VA, Kinsman OS, Marriott MS, Gomez de las Heras F, Martin JJ (1998) Antimicrob Agents Chemother 42:2279
6. Justice MC, Hsu MJ, Tse B, Ku T, Balkovec J, Schmatz D, Nielsen J (1998) J Biol Chem 273:3148
7. Justice MC, Ku T, Hsu MJ, Carniol K, Schmatz D, Nielsen J (1999) J Biol Chem 274:4869
8. Gomez-Lorenzo MG, Spahn CM, Agrawal RK, Grassucci RA, Penczek P, Chakraburtty K, Ballesta JP, Lavandera JL, Garcia-Bustos JF, Frank J (2000) EMBO J 19:2710
9. Spahn CM, Gomez-Lorenzo MG, Grassucci RA, Jorgensen R, Andersen GR, Beckmann R, Penczek PA, Ballesta JP, Frank J (2004) EMBO J 23:1008
10. Taylor DJ, Nilsson J, Merrill AR, Andersen GR, Nissen P, Frank J (2007) EMBO J 26:2421
11. Demeshkina N, Hirokawa G, Kaji A, Kaji H (2007) Nucleic Acids Res 35:4597
12. Capa L, Mendoza A, Lavandera JL, de las Heras FG, Garcia-Bustos JF (1998) Antimicrob Agents Chemother 42:2694
13. Dominguez JM, Gomez-Lorenzo MG, Martin JJ (1999) J Biol Chem 274:22423
14. Dominguez JM, Kelly VA, Kinsman OS, Marriott MS, Gomez de las Heras F, Martin JJ (1998) Antimicrob Agents Chemother 42:2274
15. Shastry M, Nielsen J, Ku T, Hsu MJ, Liberator P, Anderson J, Schmatz D, Justice MC (2001) Microbiology 147:383
16. Morris AL, MacArthur MW, Hutchinson EG, Thornton JM (1992) Proteins 12:345
17. Chen R, Li L, Weng Z (2003) Proteins 52:80
18. Frank J, Radermacher M, Penczek P, Zhu J, Li Y, Ladjadj M, Leith A (1996) J Struct Biol 116:190
19. Dundas J, Ouyang Z, Tseng J, Binkowski A, Turpaz Y, Liang J (2006) Nucleic Acids Res 34:W116
20. Gabashvili IS, Gregory ST, Valle M, Grassucci R, Worbs M, Wahl MC, Dahlberg AE, Frank J (2001) Mol Cell 8:181
21. Frank J (2006) Three-dimensional electron microscopy of macromolecular assemblies. Oxford University Press, New York
22. Roseman AM (2000) Acta Crystallogr D Biol Crystallogr 56:1332
23. Sobolev V, Eyal E, Gerzon S, Potapov V, Babor M, Prilusky J, Edelman M (2005) Nucleic Acids Res 33:W39
24. Baker NA, Sept D, Joseph S, Holst MJ, McCammon JA (2001) Proc Natl Acad Sci U S A 98:10037
25. Humphrey W, Dalke A, Schulten K (1996) J Mol Graph 14:33
26. Pettersen EF, Goddard TD, Huang CC, Couch GS, Greenblatt DM, Meng EC, Ferrin TE (2004) J Comput Chem 25:1605
27. Jorgensen R, Ortiz PA, Carr-Schmid A, Nissen P, Kinzy TG, Andersen GR (2003) Nat Struct Biol 10:379
28. Kyte J, Doolittle RF (1982) J Mol Biol 157:105
29. Okada H, Kamiya S, Shiina Y, Suwa H, Nagashima M, Nakajima S, Shimokawa H, Sugiyama E, Kondo H, Kojiri K, Suda H (1998) J Antibiot (Tokyo) 51:1081
30. Soe R, Mosley RT, Justice M, Nielsen-Kahn J, Shastry M, Merrill AR, Andersen GR (2007) J Biol Chem 282:657
31. Mitra K, Frank J (2006) Annu Rev Biophys Biomol Struct 35:299
32. Frank J, Agrawal RK (2000) Nature 406:318